

# Disentangling Fine-Tuning from Pre-Training in Visual Captioning with Hybrid Markov Logic

1<sup>st</sup> Monika Shah  
University of Memphis  
mshah2@memphis.edu

2<sup>nd</sup> Somdeb Sarkhel  
Adobe Research  
sarkhel@adobe.com

3<sup>rd</sup> Deepak Venugopal  
University of Memphis  
dvngopal@memphis.edu

**Abstract**—Multimodal systems have highly complex processing pipelines and are pretrained over large datasets before being fine-tuned for specific tasks such as visual captioning. However, it becomes hard to disentangle what the model learns during the fine-tuning process from what it already knows due to its pretraining. In this work, we learn a probabilistic model using Hybrid Markov Logic Networks (HMLNs) over the training examples by relating symbolic knowledge (extracted from the caption) with visual features (extracted from the image). For a generated caption, we quantify the influence of training examples based on the HMLN distribution using probabilistic inference. We evaluate two types of inference procedures on the MSCOCO dataset for different types of captioning models. Our results show that for BLIP2 (a model that uses a LLM), the fine-tuning may have smaller influence on the knowledge the model has acquired since it may have more general knowledge to perform visual captioning as compared to models that do not use a LLM.

**Index Terms**—Vision Large Language Model, Visual Captioning, Hybrid Markov Logic.

## I. INTRODUCTION

Image captioning is arguably one of the most popular multimodal AI applications that integrates language processing, visual understanding and knowledge representation. Well-known captioning models [25, 30] generate captions that are often similar to *ground-truth* captions written by humans. The degree of similarity is typically quantified using scores such as BLEU, CiDer, ROGUE and METEOR [3, 11, 31]. Other reference-free metrics [18, 27] attempt to analyze if the generated text describes key features in the image. A popular approach is CLIPScore [18] which embeds the generated caption and the test image into a common embedding-space using the CLIP model and evaluates the caption based on the similarity between the text and image embeddings. While all of the aforementioned methods tell us if a captioning model generates high-quality captions, they are not designed to analyze the influence of the data distribution on the outputs observed from the model.

Almost all captioning models are often *pre-trained* over very large, general datasets before they are fine-tuned with examples from a more specific target distribution. In this work we want to *disentangle what the model learns from examples from a training distribution used for fine-tuning from more general features it has learned during pre-training*. Such disentanglement can help explain if fine-tuning adds/removes/modifies

This research was supported by NSF award #2008812. The opinions, findings, and results are solely the authors' and do not reflect those of the funding agencies.

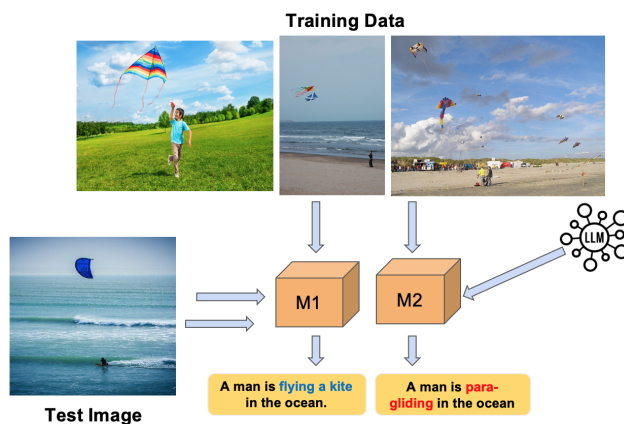


Fig. 1. Illustrative example where M2 is pretrained with an LLM while M1 is not. For M1, the source of its knowledge in generating the caption can be traced in the training examples while for M2 it is harder since it may have more general knowledge from pretraining.

knowledge acquired by the pre-trained model. For instance, suppose we consider the example in Fig. 1, the model  $M1$  generates the caption with *kite-flying* which can be observed in the training examples, but the VLLM model generates a caption with *para-gliding* that cannot be traced to examples in the training dataset used for fine-tuning.

To do this, we interpret the generated caption as a sample drawn from the training distribution. We learn this distribution based on concepts seen by the model in the training examples. To do this, we use a language called Hybrid Markov Logic Networks (HMLNs) [41], where we can define a unified distribution over symbolic constraints combined with real-valued functions. This allows us to define a distribution over text and visual modalities, i.e., we combine symbolic concepts (from text) with real-valued functions over visual features (from the image). To explain how a model learns concepts to generate a caption from this distribution, we formalize two inference tasks. The first one is *abductive inference* which is formalized as computing the Max a Posteriori (MAP) estimate. Here, conditioned on the visual features in the image, we compute if the generated caption has the maximum probability. To do this, we add constraints between concepts in the generated caption and those in the true distribution using semantic equivalence and compute the approximate MAP solution using an off-the-shelf Mixed-Integer Linear Programming (MILP)

solver. In our second inference task, we infer the probability of training examples conditioned on the generated caption. A larger probability indicates that the training instance has greater relevance to the generated caption.

We evaluate both inference methods on the MSCOCO dataset where we evaluate varied types of captioning models such as SGAE [43], transformer-based models [9, 21, 30] and BLIP2 (a Visual Large Language Model (VLLM) based model) [25]. Our results for MAP inference shows that captions generated using BLIP2 have smaller MAP probabilities compared to the other methods. We also design an Amazon Mechanical Turk (AMT) study where we ask users if contrastive training examples that have high/low probabilities w.r.t a generated caption matched with their own perception of how the model acquired knowledge for caption generation. For the case of BLIP2 generated captions, users found that the contrastive examples were less interpretable as compared to other methods. The results seem to indicate that fine-tuning may have smaller influence in a model such as BLIP2 (since it has more general knowledge through LLMs) compared to other models that did not use LLMs.

## II. RELATED WORK

There are several methods that relate visual features with the caption text to analyze the performance of captioning systems. Specifically, CLIPScore [18] uses the well-known CLIP model to embed the image and its corresponding caption to measure coherence between the two. Similarly, VIFIDEL [27] measures the visual fidelity by comparing a representation of the generated caption with the visual content. CLAIR [6] prompts a Large Language Model to score generated captions.

In [39], a probabilistic model is used to detect out of distribution (OOD) images in image captioning. In particular, several manifestations of OOD instances such as those containing novel objects, corrupted or anomalous images, low-quality images, etc. are identified with this approach. In [37], an approach to evaluate captioning models was developed from distributions learned using Markov Logic Networks (MLNs). However, unlike HMLNs, MLNs do not allow us to specify real-valued functions over visual features. More recently, a more general approach for verification of real-valued functions over embeddings by combining them with symbolic knowledge using HMLNs was proposed in [38]. However, unlike our proposed approach, the previous approaches were not designed to disentangle fine-tuning from pre-training. Our approach is also related more generally to the work in [16] which proposed an approach to quantify learning bias in a generative model.

The area of knowledge disentanglement has been studied in different contexts. In [2], an approach is proposed for disentangled knowledge acquisition in visual question answering, where the question is decomposed into sub-questions and knowledge required for each sub-question is obtained from different sources. Training Data Attribution methods have been proposed as a way to trace factual knowledge back to the training examples. This allows us to determine where a Large Language Model (LLM) acquired its knowledge from

and increases trust in the model [1]. In [42], an approach orthogonal to ours is proposed where the idea is to trace LLM capabilities back to pretraining data. This helps us understand the extent to which memorization from large-scale examples helps an LLM achieve impressive performance and the degree to which they can actually generalize.

## III. BACKGROUND

Here, we provide a brief background on HMLNs and inference using Gibbs sampling that we utilize in our approach.

### A. Hybrid Markov Logic Networks

A HMLN is a set of pairs  $(f_i, \theta_i)$ , where  $f_i$  is a First-Order Logic (FOL) formula [14] and  $\theta_i$  is a weight associated with that formula to represent its uncertainty.  $f_i$  is called a hybrid formula if it contains both continuous functions along with symbolic/discrete terms. Given a domain of constants that can be substituted for variables in the formulas, we can *ground* a formula by substituting all its variables with constants from their respective *domains*. A predicate symbol specifies a relation over terms. A *ground predicate* is one where all the variables in its arguments have been replaced by constants/objects from their respective domains.

In the HMLN distribution, a ground predicate is considered as a random variable. Ground predicates that are discrete/symbolic take values 0/1 and numeric terms take continuous values. We use the terms ground predicate or ground atom interchangeably. The value of a ground formula is equal to 0/1 if it contains no numeric terms while a ground formula with numeric terms has a continuous value.

We can represent the distribution of a HMLN as a product of potential functions, where each potential function specifies a ground formula. Specifically, the distribution takes a log-linear form where each grounding has a value equal to  $e^{\theta \times s}$ , where  $\theta$  is the weight of the formula that the potential represents and  $s$  is the value of the formula (for a purely symbolic formula this is 0/1). We can specify the product over all potentials in the distribution as follows.

$$P(\mathbf{X} = \mathbf{x}) = \frac{1}{Z} \exp \left( \sum_i \theta_i s_i(\mathbf{x}) \right) \quad (1)$$

where  $\mathbf{x}$  is a *world*, i.e., an assignment to the variables defined in the HMLN distribution,  $s_i(\mathbf{x})$  is the value of the  $i$ -th formula given the world  $\mathbf{x}$ ,  $Z$  is the normalization constant also called as the partition function which is intractable to compute since it is a summation over all possible worlds.

### B. Gibbs Sampling

We can estimate expected values from the HMLN distribution using Gibbs sampling [13], a widely used Markov Chain Monte Carlo (MCMC) algorithm. Specifically, we generate samples from the distribution  $P(\mathbf{y}|\mathbf{X})$  as follows. We start with a random assignment to all non-evidence ground predicates  $\mathbf{y}$ . In each iteration, we sample the assignment to a ground predicate  $y \in \mathbf{y}$  from a conditional distribution  $P(y|\mathbf{X}, MB(y))$ , where  $MB(y)$  denotes the Markov Blanket

of  $y$ .  $MB(y)$  is the set of ground predicates connected to  $y$  via a formula in the HMLN. Conditioning on  $MB(y)$  renders  $y$  conditionally independent of all the other variables in the HMLN and therefore, computing the conditional distribution at each iteration is very efficient. Typically, the sampler is allowed to run for a few iterations (called the *burnin* time) to allow it to *mix* which ensures that it forgets its initialization and starts to collect samples from the target distribution. We can estimate any expectation from samples drawn from the mixed sampler and as the number of samples go to  $\infty$ , the expectations converge to their true values.

#### IV. APPROACH

##### A. Notation

To formalize our approach, we use the following notation. We use upper-case letters ( $X, Y$ , etc.) to denote variables which in HMLNs are ground predicates. We use lower-case ( $x, y$ , etc.) to denote assignments on the variables. We use bold-face fonts for upper-case letters to denote multiple variables ( $\mathbf{X}, \mathbf{Y}$ , etc.) and bold-face fonts on lower-case letters to denote assignments (or a sample) over these variables ( $\mathbf{x}, \mathbf{y}$ , etc.).

##### B. HMLN Structure

We define the HMLN structure using templates of hybrid formulas. Note that the HMLN framework is flexible enough to represent arbitrary FOL structures. However, in our case, we limit the HMLN to explainable structures and therefore, similar to the approach in [41], we pre-define templates and then slot-fill the templates from training data.

**Definition 1.** A conjunctive feature ( $\mathcal{C}$ ) is a hybrid formula of the form,  $f_c(X_i, \dots, X_k) \times (X_1 \wedge X_2 \dots X_k)$ , where  $X_i$  and  $X_{i+1}$  are ground predicates that share at least one common term and  $f_c(\cdot)$  is a real-valued function, and  $\times$  indicates that we multiply the real-term with the symbolic formula.

**Definition 2.** An XOR feature ( $\mathcal{I}$ ) is defined as the XOR over a pair of ground predicates, i.e.,  $f_r(X_i, X_j) \times (X_i \wedge \neg X_j) \vee (X_j \wedge \neg X_i)$  where  $X_i, X_j$  share at least one variable between them and  $f_r(\cdot)$  is a real-valued function.

The  $\mathcal{C}$  property connects ground predicates that occur together within captions, i.e., concepts that are related to each other. The  $\mathcal{I}$  property encodes our reasoning that observing a predicate explains away the existence of the other predicate. Specifically, we can write the symbolic part of the property as  $(X_i \Rightarrow \neg X_j) \wedge (X_j \Rightarrow \neg X_i)$  if we ignore the case where the head of the implications are false.

The training data  $\mathcal{D}$  consists of image and caption pairs (where the caption is a human-written). For each image in the training data, we select its caption and extract ground predicates for this captions using a textual scene graph parser [36]. We slot-fill the  $\mathcal{C}$  template by chaining predicates with shared objects in the same image. We limit the size of the chain to a maximum of two predicates since beyond this, the chains seem to lack coherence. For each  $\mathcal{C}$  formula, we also fill its corresponding  $\mathcal{I}$  template.

**Real-Valued Terms.** The real-valued terms in definitions 1 and 2 connect the visual and text modalities. Specifically, let  $X_1, X_2$  represent two ground predicates in a formula that was extracted from  $D \in \mathcal{D}$ . We use CLIP [34] to embed the image in  $D$  and the predicates  $X_1, X_2$  into a common embedding-space. Let  $g(X_1), g(X_2)$  represent the cosine similarities between the image embedding and each of the predicate embeddings respectively. Following the semantics defined in [41], the real-valued terms in the  $\mathcal{I}$  and  $\mathcal{C}$  potentials are expressed as follows.

##### Definition 3.

$$f_c(X_1, X_2) = \min\{-\log \sigma(\epsilon - g(X_1)), -\log \sigma(\epsilon - g(X_2))\}$$

where  $\sigma$  represents the sigmoid function and  $\epsilon$  is a constant. In terms of HMLN semantics, the soft inequality  $g(X_1) \geq \epsilon$  is represented by the negative log-sigmoid of  $(\epsilon - g(X_1))$ . Thus, if the visual representation agrees with the symbolic predicates resulting in larger values of  $g(X_1), g(X_2)$ , the function assigns a higher value to the formula.

##### Definition 4.

$$f_r(X_1, X_2) = -(g(X_1) - g(X_2))^2$$

We can show that if the weight of the formula is  $\theta$ ,  $f_r(\cdot)$  is a Gaussian penalty with standard deviation  $\sqrt{1/2\theta}$ . Larger differences between  $g(X_1)$  and  $g(X_2)$  imposes a greater penalty on the  $\mathcal{I}$  formulas and thus assigns a smaller value to the formula.

Note that Lukasiewicz approximations for continuous logic [4] extends Boolean logic to the continuous case where each variable is allowed to take a continuous value in the interval  $[0, 1]$ . The Lukasiewicz t-norm and t-co-norm define  $\wedge$  and  $\vee$  operators for continuous logic. The  $\mathcal{C}$  and  $\mathcal{I}$  values can be considered as variants of this approximation. Specifically, for the  $\mathcal{C}$  value, we consider the minimum value (instead of the sum) since we want to penalize a formula even if one of its predicates is a poor descriptor for the image. Similarly, for the  $\mathcal{I}$  value, we use the Gaussian penalty instead of a simple difference between the values.

##### C. Learning

We parameterize the HMLN structure using max-likelihood estimation. However, note that in our case learning the weights for all the potential functions jointly is infeasible since the number of groundings can be extremely large. Further, to perform inference on a specific query (in our case the output produced by a model for a single test instance) note that only a small number of groundings will be relevant to the query since we can assume that the other groundings will have a value equal to 0 and thus do not influence the inference results [12]. Therefore, we instead develop an *inference guided* parameterization where we learn parameters during inference time on a subset of the HMLN formula groundings that are relevant to the inference query. Inference based learning has also been utilized to scale-up learning in large graphical

models [8]. To do this, we identify and localize objects in the image using Faster R-CNN [35] and learn query-specific parameters for potential functions that contain these objects.

**Parameterization.** The log-likelihood function for the HMLN is as follows.

$$\ell(\Theta : \mathcal{D}) = \log \frac{1}{Z(\Theta)} \exp \left\{ \sum_{i=1}^k \theta_i \mathbb{E}_{\mathcal{D}} [C_i(\mathcal{X}) + \mathcal{I}_i(\mathcal{X})] \right\} \quad (2)$$

where  $\Theta$  is the set of parameters to be learned,  $Z(\Theta)$  is the normalization constant,  $\mathbb{E}_{\mathcal{D}} [C_i(\mathcal{X}) + \mathcal{I}_i(\mathcal{X})]$  is the empirical expectation of the values in the  $i$ -th conjunctive and XOR features. Specifically, this is computed as the average value of the features over the dataset  $\mathcal{D}$ . Since the model is log-linear, the gradient of  $\ell(\Theta : \mathcal{D})$  w.r.t to the  $i$ -th weight is as follows [23].

$$\frac{\partial(\ell(\Theta : \mathcal{D}))}{\partial \theta_i} = \mathbb{E}_{\mathcal{D}} [C_i(\mathcal{X}) + \mathcal{I}_i(\mathcal{X})] - \mathbb{E}_{\Theta} [C_i(\mathcal{X}) + \mathcal{I}_i(\mathcal{X})]$$

Note that each feature consists of both real and symbolic terms. Eq. 2 corresponds to generative learning since we jointly optimize over the both terms. However, in our case, models use the image to learn relationships described in a caption. Therefore, we use discriminative learning where we condition on the real-valued terms. Let  $\mathbf{x}[m]$  denote the real-valued terms and  $\mathbf{y}[m]$  the symbolic terms for the  $m$ -th instance in the training data. The gradient of the conditional log-likelihood (CLL) is as follows.

$$\frac{\partial(\ell(\Theta : \mathcal{D}))}{\partial \theta_i} = \sum_{m=1}^M (C_i(\mathbf{y}[m], \mathbf{x}[m]) + \mathcal{I}_i(\mathbf{y}[m], \mathbf{x}[m])) - \mathbb{E}_{\Theta} [C_i(\mathbf{y}[m]|\mathbf{x}[m]) + \mathcal{I}_i(\mathbf{y}[m]|\mathbf{x}[m])]) \quad (3)$$

Though the CLL is concave and thus has a globally optimal parameterization, there is no analytical closed form solution. Therefore, we use iterative methods such as gradient ascent to maximize the CLL. However, this leads to a complication. Note that to compute the expected value of a feature, we need to compute the exact marginal probability of each feature which is intractable since the normalization constant is unknown. Therefore, we use contrastive divergence [19] to approximate the expectation. Specifically, the idea is to draw samples from the distribution using the weights estimated thus far and estimate the expected value of a feature as a Monte-Carlo estimate over the samples. Note that since we need only the approximate gradient direction, a few samples are sufficient to perform the weight update efficiently. To do this, we use Gibbs sampling to generate the samples and compute the expected value of a feature as the average value computed over the samples. Note that we can update the weights of all the features in parallel by jointly sampling  $\mathbf{y}[m]$  given  $\mathbf{x}[m]$  for all  $m$ . Algorithm 1 summarizes our parameter learning approach.

---

### Algorithm 1: Parameter Learning

---

**Input:** Query specific HMLN structure  $\mathcal{H}$ , Training data  $\mathcal{D}$ , learning rate  $\eta$

**Output:** Learned weights  $\{\theta_i\}_{i=1}^k$   
// Contrastive Divergence

```

1 Initialize weights  $\{\theta_i^{(0)}\}$ 
2 for  $t$  from 1 to  $T$  do
3    $\{\mathbf{x}^{(t)}, \mathbf{y}^{(t)}\} =$  Sample from  $\mathcal{H}$  parameterized with
    $\{\theta_i^{(t-1)}\}_{i=1}^k$  using Gibbs sampling
4   for each weight  $\theta_i$  in  $\mathcal{H}$  do
5     Estimate the expected value in Eq. (3) from
    $\{\mathbf{x}^{(t)}, \mathbf{y}^{(t)}\}$ 
6      $\frac{\partial(\ell(\Theta, \mathcal{D}))}{\partial \theta_i^{(t)}}$  = Gradient computed using Eq. (3)
7     Update  $\theta_i^{(t)} = \theta_i^{(t-1)} + \eta * \frac{\partial(\ell(\Theta, \mathcal{D}))}{\partial \theta_i^{(t)}}$ 
8 return  $\{\theta_i^{(T)}\}_{i=1}^k$ 

```

---

### D. Abductive Inference

Abduction in logical reasoning is typically useful in finding the most likely explanation for an observation. In a probabilistic model, this is equivalent to the *Max a Posteriori* (MAP) reasoning task. Specifically, given some observed evidence, the MAP solution finds an explanation that maximizes the joint probability over all variables in the model. To formalize this, let  $\mathbf{Y}^*[m]$  be the ground predicates from a human-written caption for image  $m$  and  $\mathbf{Y}[m]$  be the ground predicates generated by a model for the same image (going forward, we drop the subscript  $m$  for readability). We want to infer if  $\mathbf{Y}^*$  is the most likely explanation for the model to generate  $\mathbf{Y}$ .

Let  $\mathbf{M}$  represent all the variables in the model and  $\mathbf{Y}^* \subseteq \mathbf{M}$ ,  $\mathbf{Y} \subseteq \mathbf{M}$ . Given an assignment to  $\mathbf{Y}$  and the visual features from the image  $\mathbf{X}$ , the MAP predicates are  $\hat{\mathbf{M}} = \mathbf{M} \setminus \mathbf{Y}$ ,  $\mathbf{X}$ . The MAP inference task is to find an assignment to  $\hat{\mathbf{M}}$  that maximizes the un-normalized log probability as follows.

$$\arg \max_{\hat{\mathbf{m}} \in \Omega(\hat{\mathbf{M}})} \exp \left( \sum_i \theta_i s_i(\hat{\mathbf{m}}, \mathbf{Y}, \mathbf{X}) \right) \quad (4)$$

where  $\Omega(\hat{\mathbf{M}})$  is the set of all possible assignments to  $\hat{\mathbf{M}}$  and  $s_i(\cdot)$  is the value  $C_i(\cdot) + \mathcal{I}_i(\cdot)$ .

**Semantic Equivalence Constraints.** To encourage the MAP solution to take into account semantic equivalences between concepts in  $\mathbf{Y}^*$  and  $\mathbf{Y}$ , we add pairwise *virtual evidence* (or soft evidence) between the predicates in  $\mathbf{Y}^*$  and  $\mathbf{Y}$ . The concept of virtual evidence was first introduced by Pearl [33] to handle uncertainty in observations. Further, this has been used in several approaches since such as semi-supervised learning [22] and grounded learning [32] as a form of indirect supervision (e.g. label preferences). In general, the idea of virtual evidence is to introduce a potential function over the evidence that encodes its uncertainty. In our case, we add the evidence based on semantic equivalence between the subject and object mentions in the predicates  $Y^* \in \mathbf{Y}^*$  and  $Y \in \mathbf{Y}$  respectively. This is similar to the approach used in [5] to add soft distributional semantics constraints to infer text

---

**Algorithm 2: Abductive Inference**

---

**Input:** Parameterized HMLN with structure  $\mathcal{H}$  and weights  $\Theta$ , ground predicates from reference captions  $\mathbf{Y}^*$ , ground predicates from generated caption  $\mathbf{Y}$   
**Output:** Assignment to MAP predicates  $\hat{\mathbf{M}}$ , MAP Objective Value  $m^*$

```
// MILP Encoding
1 for each formula f with parameter theta in H do
2   X = Continuous terms in f
3   Y = Discrete Terms in f
4   Add X, Y to MILP model
5   Add hard constraint f ⇔ a, where a is an auxiliary
   variable with objective theta
// Soft Evidence
6 for (Y, Y*), where Y ∈ Y, Y* ∈ Y* do
7   S = Similarity between subjects in Y, Y*
8   O = Similarity between objects in Y, Y*
9   Add hard constraint (Y ⇔ Y*) ⇔ â, where â is an
   auxiliary variable with objective min(S, O)
10 m̂, m* = Assignment and objective value solving Eq. (4)
   using a MILP solver
11 return m̂, m*
```

---

entailment. Specifically, we use a standard word embedding model to compute the similarity scores between the subject pairs in  $(Y^*, Y)$  and the object pairs in  $(Y^*, Y)$ . We consider the semantic equivalence score  $S(Y^*, Y)$  as the minimum of the two similarity scores. We add the virtual evidence  $(Y^* \Leftrightarrow Y)$  with value equal to  $S(Y^*, Y)$ .

**MILP Encoding.** Computing the exact MAP solution that optimizes Eq. (4) is known to be NP-hard [23]. Therefore, we compute the approximate MAP solution with the help of a Mixed Integer Linear Programming (MILP) solver. The encoding that we use is as follows. Each symbolic feature is represented as a binary variable and a continuous feature is encoded as a real-valued variable. We introduce auxiliary variables for each formula and also for the soft evidence. Specifically, for a formula  $f$  (or soft evidence) with weight  $\theta$ , we introduce a binary auxiliary variable  $a$  with objective  $\theta$  and add a hard constraint  $f \Leftrightarrow a$  which is encoded as linear constraints in the MILP. In our experiments, we use a state-of-the-art solver namely, Gurobi [17] to compute the MAP solution efficiently. Larger MAP objective values indicate that the explanation of the evidence (visual features of the image and ground predicates in human-written captions) using the generated caption is more likely in the HMLN distribution. Algorithm 2 summarizes our MAP inference approach.

### E. Back-Tracing Captions to Training Examples

The MAP inference approach proposed in the prior section requires reference (human written) captions for test images. Therefore, for large-scale datasets, this becomes harder to scale. We next develop an approach where we do not use reference captions but instead explain the bias in the generated caption through examples from the training data. First, we formalize bias similar to its formalization in a generative model [16]. Specifically, given the true distribution  $P(\cdot)$ ,

suppose the model generates a sample  $\mathbf{y}$  from  $P_\phi(\cdot)$ , we can quantify the bias in the generative distribution with the following ratio.

$$w(\mathbf{y}) = \frac{P(\mathbf{y})}{P_\phi(\mathbf{y})} \quad (5)$$

The ratio in Eq. (5) is also called as the *importance weight* of a sample drawn from  $P_\phi(\cdot)$  when the true distribution is  $P(\cdot)$ . This is commonly used in importance sampling [26] where samples drawn from a proposal distribution  $P_\phi(\cdot)$  are used to estimate expectations over  $P(\cdot)$ . The closer  $P_\phi(\cdot)$  is to  $P(\cdot)$ , samples from  $P_\phi(\cdot)$  have smaller bias.

We apply importance weighting in our approach as follows. Let  $\mathbf{Y}$  be the ground predicates extracted from the generated caption and let  $P(\mathbf{Y}|\mathbf{X})$  represent the distribution over the ground predicates conditioned on the visual features  $\mathbf{X}$  of the test image. Let  $\hat{\mathbf{X}}$  be the visual features from a training image. Given an sample  $\mathbf{y}$  from  $P(\mathbf{Y}|\mathbf{X})$ , its importance weight is defined as follows.

$$w(\mathbf{y}) = \frac{P(\mathbf{y}|\hat{\mathbf{X}})}{P(\mathbf{y}|\mathbf{X})} \quad (6)$$

**Marginal Density Estimation.** We estimate the marginal densities over training examples using the importance weights. However, the number of training examples is typically very large. Further, most of the training examples will typically have little relevance to a test example. Therefore, to scale-up we first select a small number of training examples that are *contextually relevant* to the test example. To do this, we only consider a training example  $\mathcal{X} \in \mathcal{D}$  that is grounded in the same context as the test image. Specifically, we consider  $\mathcal{X}$  to be contextually relevant to a test example  $\mathcal{Y}$  iff for each ground predicate  $X$  from the caption for  $\mathcal{X}$ , there exists a ground predicate  $Y$  in the generated caption for  $\mathcal{Y}$  such that  $S(X, Y) > C$ , where  $S(X, Y)$  is the score measuring semantic equivalence between  $X$  and  $Y$ , and  $C$  is a constant.

Let  $\mathcal{X}$  be a training image that is contextually relevant to the test image and let  $\mathbf{Y}$  be ground predicates in the generated caption. The density  $P(\mathcal{X}|\mathbf{Y})$  is the likelihood that a model that learns from  $\mathcal{X}$  has generated  $\mathbf{Y}$ . We assume a *mean-field* distribution over all related training examples and therefore in factorized form, we can write its joint distribution as follows.

$$P(\mathcal{X}_1 \dots \mathcal{X}_n | \mathbf{Y}) = \prod_{i=1}^n P(\mathcal{X}_i | \mathbf{Y}) \quad (7)$$

Given a sample  $\mathbf{y}$  over the ground predicates, we define the following indicator function.  $\mathbb{I}_{\mathcal{X}}[\mathbf{y}] = 1$  iff  $\mathbf{y}$  contains an assignment to predicates such that for each predicate that exists in  $\mathcal{X}$ , there is a semantically equivalent predicate that has an assignment equal to 1 in  $\mathbf{y}$ . We can compute the expected value of the indicator function using importance weights as follows.

$$\mathbb{E}_{\mathbf{y} \sim P(\mathbf{Y}|\hat{\mathbf{X}})} [\mathbb{I}_{\mathcal{X}}[\mathbf{y}]] = \mathbb{E}_{\mathbf{y} \sim P(\mathbf{Y}|\mathbf{X})} \left[ \frac{P(\mathbf{y}|\hat{\mathbf{X}})}{P(\mathbf{y}|\mathbf{X})} \mathbb{I}_{\mathcal{X}}[\mathbf{y}] \right]$$

Since computing the exact expectation is intractable, given  $T$  samples  $\mathbf{y}_1 \dots \mathbf{y}_T$ , we can obtain a Monte-Carlo estimate of the expected value as follows.

$$\mathbb{E}_{\mathbf{y} \sim P(\mathbf{Y}|\hat{\mathbf{X}})} [\mathbb{I}_{\mathcal{X}}[\mathbf{y}]] \approx \frac{1}{T} \sum_{i=1}^T w(\mathbf{y}_i) \mathbb{I}_{\mathcal{X}}[\mathbf{y}_i] \quad (8)$$

Thus, using samples drawn from  $P(\mathbf{Y}|\hat{\mathbf{X}})$ , we can estimate the expectation in Eq. (8). From the results in [26], we can show that the estimator is unbiased, i.e., we can show that as  $T \rightarrow \infty$ , the estimates converge to the true expectation. However, a technical challenge is that it is hard to estimate the true importance weights. Specifically, note that the distributions in the numerator and denominator in Eq. (6) have different normalization constants. Therefore, to estimate the exact weights, we need to estimate the normalization constants of both the distributions which is computationally intractable. Therefore, we instead use an approximate estimator where it is tractable to estimate the importance weights. Specifically, we compute the ratio of the un-normalized probabilities to compute the weights. In this case, the computation is efficient since we do not need the normalization constants. Thus, we have a modified weight as follows.

$$w(\mathbf{y}) \propto \frac{P(\mathbf{y}|\hat{\mathbf{X}})}{P(\mathbf{y}|\mathbf{X})} \quad (9)$$

We can show that using the weights in Eq. (9), the estimated expectation is *asymptotically unbiased* [26], i.e., the bias goes to 0 as  $T \rightarrow \infty$ . A second practical difficulty is that some weights may get too large and this tends to yield poor estimates. To ensure that weights do not get too large, we use an approach called *clipping* which thresholds the maximum weights. This ensures that a few weights do not dominate in the estimation of the expectation. The modified estimator combining the un-normalized weights and clipping is as follows.

$$P(\mathcal{X}|\mathbf{Y}) \approx \frac{\sum_{i=1}^T \max(w(\mathbf{y}_i, 1)) \mathbb{I}_{\mathcal{X}}[\mathbf{y}_i]}{\sum_{i=1}^T \max(w(\mathbf{y}_i, 1))} \quad (10)$$

As  $T \rightarrow \infty$ , the estimate of the expectation computed in Eq. (10) converges to true marginal density  $P(\mathcal{X}|\mathbf{Y})$ . To implement this, we use Gibbs sampling. Specifically, we perform Gibbs sampling to draw samples from  $P(\mathbf{y}|\mathbf{X})$  and weight each sample by computing the unnormalized ratio in Eq. (9). Strictly speaking, for the estimator in Eq. (10), we would want the samples drawn from  $P(\mathbf{y}|\mathbf{X})$  to be independent of each other. However, Gibbs sampling generates dependent samples. That is, the sample generated in an iteration depends upon previous samples. To address this, we use a technique called *thinning*, where we only consider samples for estimating the weight after every  $k$  Gibbs iterations. This reduces the dependence among samples.

**Contrastive Samples.** Humans often compare contrastive examples to understand concepts [28]. Therefore, in our case, we use the distribution in Eq. (7) to sample instances that have contrasting influence on the generated caption. Specifically, the

---

### Algorithm 3: Marginal Inference

---

**Input:** Ground predicates from generated caption  $\mathbf{Y}$ , relevant training examples  $\{\mathcal{X}_i\}_{i=1}^n$   
**Output:** Contrastive training samples for  $\mathbf{Y}$

- 1 **for each** Gibbs sample  $\mathbf{y}^{(t)}$  from the target distribution  $P(\mathbf{Y}|\mathbf{X})$  **do**
- 2     Compute the un-normalized sample weight  $w(\mathbf{y}^{(t)})$  using Eq. (9)
- 3     **for each**  $\mathcal{X}_i$  **do**
- 4         Update its marginal density using the estimator in Eq. (10)
- 5 **return**  $\arg \max_{i=1}^n \hat{P}(\mathcal{X}_i)$ ,  $\arg \min_{i=1}^n \hat{P}(\mathcal{X}_i)$

---

minimal factor in the distribution,  $\mathcal{X}^- = \arg \min_{i=1}^n P(\mathcal{X}_i|\mathbf{Y})$  denotes the training instance that is the least likely to generate  $\mathbf{Y}$ . The maximal factor  $\mathcal{X}^+ = \arg \max_{i=1}^n P(\mathcal{X}_i|\mathbf{Y})$  denotes the most likely instance to generate  $\mathbf{Y}$ . Algorithm 3 summarizes our approach.

## V. EXPERIMENTS

### A. Implementation

To implement our approach, we used the textual scene graph parser [36] to obtain ground predicates from the text of captions. We used the pretrained CLIP model to embed the image and text to encode real-valued terms in the HMLN. For weight learning in the HMLN, we set the learning rate to 0.01. To implement abductive inference, we used the MILP solver in Gurobi to obtain the approximate MAP solution. For determining semantic equivalence between ground predicates, we used SpaCy word embedding similarity scores [20]. For the Gibbs sampler, we used a *burn-in* of 500 samples. After this, we estimated the marginal probabilities using the clipped estimator with an interval of 10 iterations between samples to minimize dependency across samples. We performed our experiments on a 62.5 GiB RAM, 64-bit Intel® Core™ i9-10885H CPU @ 2.40GHz × 16 processor with a NVIDIA Quadro GPU with 16GB RAM. Our code is available at the following link. <https://github.com/Monikshah/caption-explanation-hmln>

### B. Models

We evaluate our approach on the state-of-the-art image captioning models including SGAE [43], AoA [21], XLAN [30], M2 [9] and Blip2 [25]. In each case, we used their publicly available models for the evaluation. Each of these models have been pretrained over datasets. Specifically, SGAE and XLAN are pretrained using ImageNet (IN) [10] and Visual Genome (VG) [24], AoA and M2 are pretrained with VG. BLIP2 is pretrained with the LLM OPT [44]. It is also pretrained with datasets VG, CC3M [40], CC12M [7] and SBU [29]). All the models are fine-tuned for generating captions on the MSCOCO image captioning benchmark dataset with Karpathy’s train, test, validation split. We use the same split to learn our HMLN and perform evaluation on the test split.

### C. MAP Inference

The average MAP objective value over captions generated for the test set is compared over all five models in Fig. 2. A larger average MAP value (smaller negative-log value) indicates that the generated captions from the model are more likely to have maximal probability in the distribution. Note that for the VLLM model BLIP2, the LLM improves general knowledge that improves captioning ability of the model. However, the generation is harder to explain with the training distribution. This trade-off can be illustrated in our results. Specifically, we compute the average rank for a model based on 5 standard captioning metrics (BLEU4, METEOR, ROUGE, CiDER and SPICE) which indicate caption quality. The ranking is indicated in Fig. 2, where BLIP2 has the highest rank followed by XLAN. However, XLAN has a significantly higher MAP value than BLIP2. Note that the other non-VLLM models with similar pretraining as XLAN have smaller MAP values since their generated captions do not explain the visual features as accurately as the captions generated by XLAN.

Some illustrative examples are shown in Fig. 3. VLLMs encode more general knowledge that can help it generate captions for test examples that are hard to learn from training examples. For instance, in Fig. 3 (a), it is hard to infer the *refrigerator* in the image, however the logo *GE* is visible and using pretraining from LLMs, BLIP2 can make the inference that it represents a refrigerator while a non-VLLM cannot. However, the smaller MAP score shows that explaining such inference is harder for VLLMs. On the other hand, for examples Fig. 3 (b), (c) the MAP values are high for both BLIP2 and the non-VLLM. However, BLIP2 includes more details within the caption (e.g. *basil, cactus*). In Fig. 3 (d), BLIP2’s LLM-based knowledge has the opposite effect since it infers that the bottle is a *fire extinguisher* due to its color. In Fig. 3 (e), the smaller MAP score for both the VLLM and non-VLLM model indicates that it is hard to explain the image using training data due to its unique characteristics (an unusual *flying kite*). Finally, in Fig. 3 (f), BLIP2 can identify the banana in a novel context compared to the non-VLLM and since this explains the visual features in the image, MAP inference reflects this in its larger value.

### D. AMT Study

We evaluate if for a generated caption by a model we can sample training examples that can help support the knowledge required for its generation. To do this, we designed an AMT study as follows. For a given test image and caption generated by a model, we provided users with training examples with contrastive probabilities selected by our approach. We asked users to rate on a Likert scale (1-5) if the explanation matched with their own perception of how the model generates its caption by learning concepts from the positive training example and contrasting it with similar concepts shown in the negative training example.

We used a total of 1000 AMT workers to obtain responses. Each explanation was given by 5 different workers. The results on captions generated from the 5 different models are shown

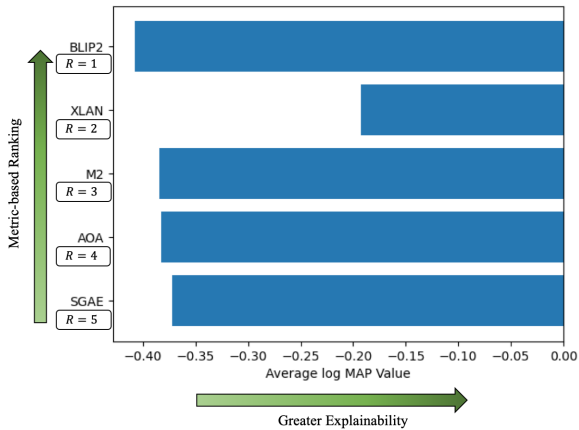


Fig. 2. The x-axis shows the average log MAP objective value computed across test images. The y-axis shows the ranking of a model where the rank is computed based on the average rank across 5 standard captioning metrics ( $R = 1$  is the highest ranked model).

TABLE I  
PAIRED T-TEST RESULTS, VALUES IN RED WERE NOT STATISTICALLY SIGNIFICANT ( $p > 0.05$ ).

	AoA	M2	XLAN	SGAE	Blip2
<b>AoA</b>		2.087	0.912	3.008	0.464
<b>M2</b>			0.78	-1.9	2.650
<b>XLAN</b>				1.2	3.579
<b>SGAE</b>					1.286

in Fig. 4. For XLAN, the users were more sure (rating 5) that the presented examples supported the generated caption compared to BLIP2. This observation is consistent with the MAP results and shows that the use of LLMs makes it harder in BLIP2 to back-trace where it acquired its knowledge from.

We also performed the paired t-test to check if the difference in responses were statistically significant. Table I shows these results and as we see, the response differences were statistically significant for most pairs except when we paired M2 captions with SGAE. Further, the responses for the BLIP2 model was significantly different from all the non-VLLM models which indicates the distinction between how VLLMs learn from the training examples compared to non-VLLM models.

### E. Analyzing the Distribution

We analyze the difference between marginal probabilities of the contrasting training examples selected by our explainer. Specifically, we compare this difference to the similarity between the test image embedding and the *ground-truth* (human-written) caption’s text embeddings computed using CLIP. To measure the distance between distributions, we use the Hellinger’s distance [15] (a symmetric distance between probability distributions) between the marginal probabilities for the contrastive examples. We expect that when the text and image have greater similarity, this implies that the training examples should be able to help learn concepts more reliably and therefore, the distance between distributions should be

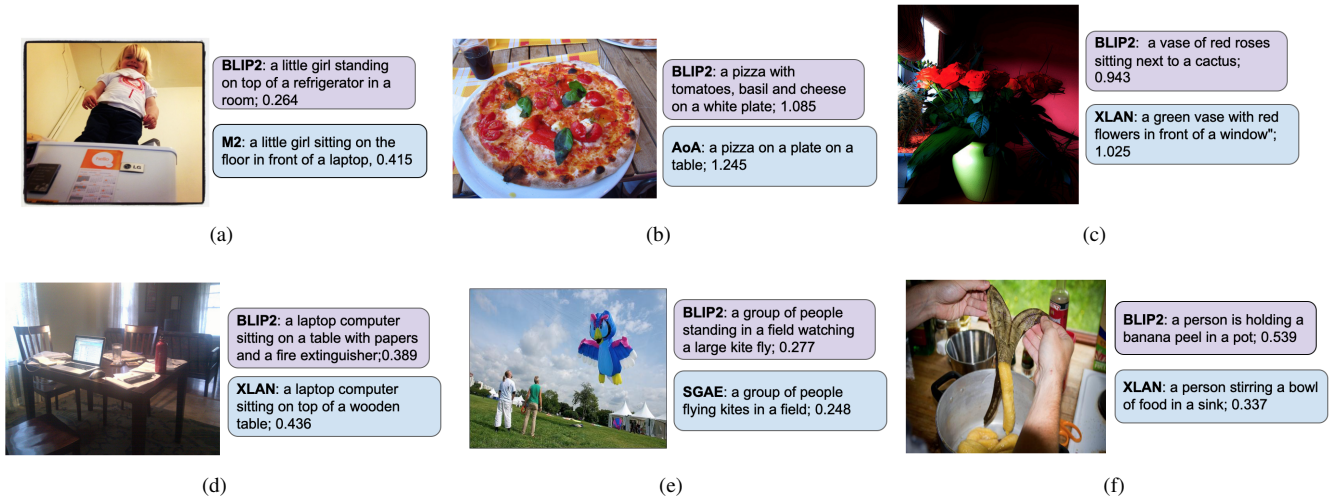


Fig. 3. Illustrative examples for MAP values of captions for BLIP2 and non-VLLM models.

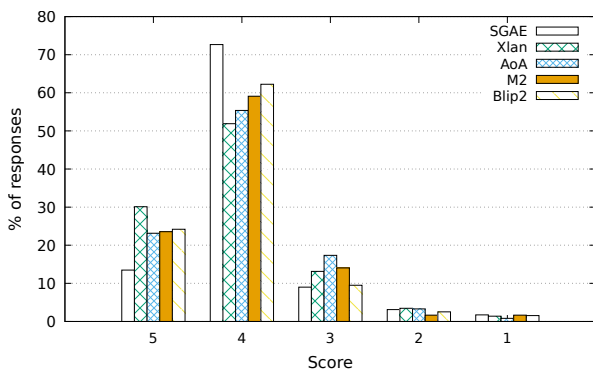


Fig. 4. Comparing responses (from a Likert scale of 1-5) from AMT users across models for explaining their generated captions using training examples. Higher values indicate that the users more strongly agreed with the explanations.

larger. The results are shown in Fig. 6. As seen in these results, out of all the models, for the VLLM BLIP2, the difference in distributions seems less explainable where in many test images, larger semantic similarity between the embeddings does not imply that the difference in distributions is large. Thus, while external sources help in caption generation with novel concepts, it does makes disentangling what is learned in fine-tuning harder.

## VI. CONCLUSION

To better understand the knowledge acquired in fine-tuning versus that acquired during pre-training, we developed a probabilistic model (HMLN) that combines visual and symbolic features from the training instances used for fine-tuning. We then developed two inference tasks where we estimate if the generated caption can be supported by the training data distribution. We performed experiments on MSCOCO on different types of visual captioning models and showed that for BLIP2 which uses a LLM within the model, it can be

harder to find support for its caption generation within the fine-tuning examples compared to other approaches that do not use LLMs. In future, we plan to generalize our work across different VLLMs and also across different multimodal tasks such as Visual Question Answering.

## REFERENCES

- [1] Ekin Akyürek, Tolga Bolukbasi, Frederick Liu, Binbin Xiong, Ian Tenney, Jacob Andreas, and Kelvin Guu. Towards tracing knowledge in language models back to the training data. In *Findings of the Association for Computational Linguistics: EMNLP 2022*, pages 2429–2446, 2022.
- [2] Wenbin An, Feng Tian, Jiahao Nie, Wenkai Shi, Haonan Lin, Yan Chen, QianYing Wang, Yaqiang Wu, Guang Dai, and Ping Chen. Knowledge acquisition disentanglement for knowledge-based visual question answering with large language models. *arXiv preprint arXiv:2407.15346*, 2024.
- [3] Peter Anderson, Basura Fernando, Mark Johnson, and Stephen Gould. Spice: Semantic propositional image caption evaluation. In *ECCV*, 2016.
- [4] Stephen H Bach, Matthias Broecheler, Bert Huang, and Lise Getoor. Hinge-loss markov random fields and probabilistic soft logic. *Journal of Machine Learning Research*, 18(109):1–67, 2017.
- [5] Islam Beltagy, Stephen Roller, Gemma Boleda, Katrin Erk, and Raymond J. Mooney. Utehas: Natural language semantics using distributional semantics and probabilistic logic. In *SemEval@COLING 2014*, pages 796–801, 2014.
- [6] David Chan, Suzanne Petryk, Joseph Gonzalez, Trevor Darrell, and John Canny. CLAIR: Evaluating image captions with large language models. In *EMNLP*, pages 13638–13646, 2023.



Fig. 5. Illustrative contrastive training examples for the generated captions. The caption shown in each case was generated for the first image, the second image is the largest probability example and the third one is the smallest probability training example.

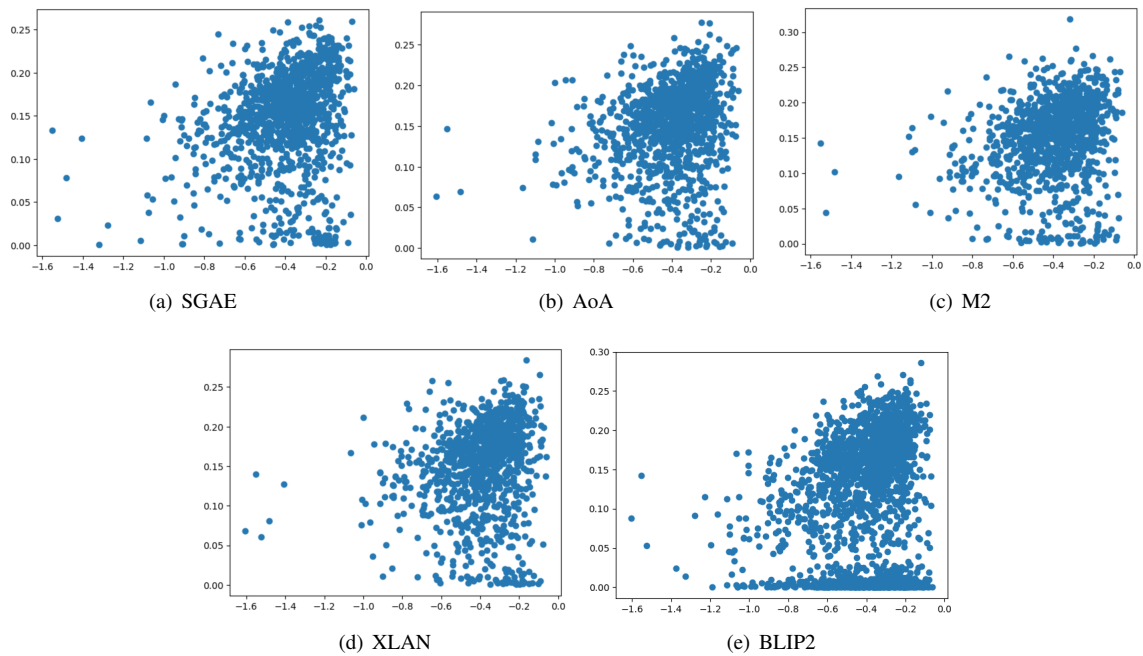


Fig. 6. The Y-axis shows the Hellinger's distance between the distributions for contrastive examples and the X-axis shows the negative log-sigmoid of the average similarity between CLIP embeddings for test images and human-written captions (closer to 0 means semantically closer).

[7] Soravit Changpinyo, Piyush Sharma, Nan Ding, and Radu Soricut. Conceptual 12m: Pushing web-scale image-text pre-training to recognize long-tail visual concepts. In *CVPR*, pages 3558–3568, 2021.

[8] Anton Checheta and Carlos Guestrin. Focused belief propagation for query-specific inference. In *AISTATS*, pages 89–96, 2010.

[9] Marcella Cornia, Matteo Stefanini, Lorenzo Baraldi, and Rita Cucchiara. Meshed-memory transformer for image captioning. In *CVPR*, pages 10578–10587, 2020.

[10] Jia Deng, Wei Dong, Richard Socher, Li-Jia Li, Kai Li, and Li Fei-Fei. Imagenet: A large-scale hierarchical image database. In *CVPR*, pages 248–255, 2009.

[11] Michael Denkowski and Alon Lavie. Meteor universal: Language specific translation evaluation for any target language. In *Workshop on Statistical Machine Translation*, 2014.

[12] Pedro Domingos and Daniel Lowd. Markov logic: An interface layer for artificial intelligence. *Synthesis lectures on artificial intelligence and machine learning*, 3(1):1–155, 2009.

[13] Stuart Geman and Donald Geman. Stochastic relaxation, gibbs distributions, and the bayesian restoration of images. *IEEE Transactions on pattern analysis and machine intelligence*, (6):721–741, 1984.

[14] Michael Genesereth and Eric Kao. Introduction to logic. *Synthesis Lectures on Computer Science*, 4(1):1–165, 2013.

- [15] Víctor González-Castro, Rocío Alaiz-Rodríguez, and Enrique Alegre. Class distribution estimation based on the hellinger distance. *Information Sciences*, 218:146–164, 2013.
- [16] Aditya Grover, Jiaming Song, Ashish Kapoor, Kenneth Tran, Alekh Agarwal, Eric Horvitz, and Stefano Ermon. Bias correction of learned generative models using likelihood-free importance weighting. In *NeurIPS*, pages 11056–11068, 2019.
- [17] Gurobi Optimization, LLC. Gurobi Optimizer Reference Manual, 2024. URL <https://www.gurobi.com>.
- [18] Jack Hessel, Ari Holtzman, Maxwell Forbes, Ronan Le Bras, and Yejin Choi. Clipscore: A reference-free evaluation metric for image captioning. In *EMNLP*, 2021.
- [19] Geoffrey E Hinton. Training products of experts by minimizing contrastive divergence. *Neural Computation*, 14(8):1771–1800, 2002.
- [20] Matthew Honnibal, Ines Montani, Sofie Van Landeghem, Adriane Boyd, et al. spacy: Industrial-strength natural language processing in python. 2020.
- [21] Lun Huang, Wenmin Wang, Jie Chen, and Xiao-Yong Wei. Attention on attention for image captioning. In *ICCV*, pages 4633–4642, 2019.
- [22] Durk P Kingma, Shakir Mohamed, Danilo Jimenez Rezende, and Max Welling. Semi-supervised learning with deep generative models. *NeurIPS*, 2014.
- [23] D. Koller and N. Friedman. *Probabilistic Graphical Models: Principles and Techniques*. MIT Press, 2009.
- [24] Ranjay Krishna, Yuke Zhu, Oliver Groth, Justin Johnson, Kenji Hata, Joshua Kravitz, Stephanie Chen, Yannis Kalantidis, Li-Jia Li, David A Shamma, et al. Visual genome: Connecting language and vision using crowd-sourced dense image annotations. *International journal of computer vision*, 123:32–73, 2017.
- [25] Junnan Li, Dongxu Li, Silvio Savarese, and Steven Hoi. Blip-2: Bootstrapping language-image pre-training with frozen image encoders and large language models. In *ICML*, pages 19730–19742, 2023.
- [26] J. S. Liu. *Monte Carlo Strategies in Scientific Computing*. Springer Publishing Company, Incorporated, 2001.
- [27] Pranava Madhyastha, Josiah Wang, and Lucia Specia. VIFIDEL: evaluating the visual fidelity of image descriptions. In *ACL*, 2019.
- [28] Tim Miller. Explanation in artificial intelligence: Insights from the social sciences. *Artificial intelligence*, 267:1–38, 2019.
- [29] Vicente Ordonez, Girish Kulkarni, and Tamara Berg. Im2text: Describing images using 1 million captioned photographs. *Advances in neural information processing systems*, 24, 2011.
- [30] Yingwei Pan, Ting Yao, Yehao Li, and Tao Mei. X-linear attention networks for image captioning. In *CVPR*, pages 10971–10980, 2020.
- [31] Kishore Papineni, Salim Roukos, Todd Ward, and Wei-Jing Zhu. Bleu: a method for automatic evaluation of machine translation. In *ACL*, pages 311–318, 2002.
- [32] Ankur Parikh, Hoifung Poon, and Kristina Toutanova. Grounded semantic parsing for complex knowledge extraction. In *NAACL*, pages 756–766, 2015.
- [33] Judea Pearl. *Probabilistic Reasoning in Intelligent Systems: Networks of Plausible Inference*. Morgan Kaufmann Publishers Inc., 1988.
- [34] Alec Radford, Jong Wook Kim, Chris Hallacy, Aditya Ramesh, Gabriel Goh, Sandhini Agarwal, Girish Sastry, Amanda Askell, Pamela Mishkin, Jack Clark, et al. Learning transferable visual models from natural language supervision. In *ICML*, pages 8748–8763, 2021.
- [35] Shaoqing Ren, Kaiming He, Ross Girshick, and Jian Sun. Faster r-cnn: Towards real-time object detection with region proposal networks. In *NeurIPS*, pages 91–99, 2015.
- [36] Sebastian Schuster, Ranjay Krishna, Angel Chang, Li Fei-Fei, and Christopher D Manning. Generating semantically precise scene graphs from textual descriptions for improved image retrieval. In *Workshop on vision and language*, 2015.
- [37] Monika Shah, Somdeb Sarkhel, and Deepak Venugopal. Evaluating captioning models using markov logic networks. In *IEEE International Conference on Big Data*, pages 127–134, 2022.
- [38] Anup Shakya, Abisha Thapa Magar, Somdeb Sarkhel, and Deepak Venugopal. On the verification of embeddings with hybrid markov logic. In *IEEE International Conference on Data Mining, ICDM 2023*, pages 1301–1306, 2023.
- [39] Gal Shalev, Gabi Shalev, and Joseph Keshet. A baseline for detecting out-of-distribution examples in image captioning. In *ACM International Conference on Multimedia*, pages 4175–4184, 2022.
- [40] Piyush Sharma, Nan Ding, Sebastian Goodman, and Radu Soricut. Conceptual captions: A cleaned, hypertexted, image alt-text dataset for automatic image captioning. In *ACL*, pages 2556–2565, 2018.
- [41] Jue Wang and Pedro M Domingos. Hybrid markov logic networks. In *AAAI*, pages 1106–1111, 2008.
- [42] Xinyi Wang, Antonis Antoniadis, Yanai Elazar, Alfonso Amayuelas, Alon Albalak, Kexun Zhang, and William Yang Wang. Generalization v.s. memorization: Tracing language models’ capabilities back to pretraining data, 2024.
- [43] Xu Yang, Kaihua Tang, Hanwang Zhang, and Jianfei Cai. Auto-encoding scene graphs for image captioning. In *CVPR*, 2019.
- [44] Susan Zhang, Stephen Roller, Naman Goyal, Mikel Artetxe, Moya Chen, Shuohui Chen, Christopher Dewan, Mona Diab, Xian Li, Xi Victoria Lin, et al. Opt: Open pre-trained transformer language models. *arXiv preprint arXiv:2205.01068*, 2022.